Open Access Library Journal
2022, Volume 9, e9556
ISSN Online: 2333-9721
ISSN Print: 2333-9705

Application of Fluid Inclusions in Reservoir Formation: A Case Study of Qilicun Oilfield in Ordos Basin

Jingwen Zhu[1,2], Shanshan Chen[1,2], Yuxuan Zhang[1,2]

[1]School of Earth Sciences and Engineering, Xi'an Shiyou University, Xi'an, China
[2]Shaanxi Key Laboratory of Petroleum Accumulation Geology, Xi'an, China
Email: 836220662@qq.com

How to cite this paper: Zhu, J.W., Chen, S.S. and Zhang, Y.X. (2022) Application of Fluid Inclusions in Reservoir Formation: A Case Study of Qilicun Oilfield in Ordos Basin. *Open Access Library Journal*, **9**: e9556.
https://doi.org/10.4236/oalib.1109556

Received: November 10, 2022
Accepted: December 27, 2022
Published: December 30, 2022

Copyright © 2022 by author(s) and Open Access Library Inc.
This work is licensed under the Creative Commons Attribution International License (CC BY 4.0).
http://creativecommons.org/licenses/by/4.0/
Open Access

Abstract

The formation time of the Chang 6 reservoir was determined semi-quantitatively by petrographic observation, fluorescence spectral analysis, homogeneous temperature test and salinity calculation of fluid inclusions in the Chang 6 reservoir of the Qilicun oilfield, as well as sonic time difference method to recover the stripping thickness of the strata at the end of the Early Cretaceous, based on the study method of burial-thermal evolution history map with homogeneous temperature cast points of inclusions. The results show that brine inclusions, gas-liquid brine inclusions and a few oil inclusions are mainly distributed in quartz healing microfractures and some feldspar grains, mainly oval or irregular in shape, with sizes ranging from 3 to 10 μm. The fluorescence colors of oil inclusions are mainly yellowish green and green; the fluorescence spectra of oil inclusions are similar to those of hydrocarbon associated brine inclusions. The analysis of the uniform temperature, salinity and burial history of the oil inclusions indicates that the oil reservoir in the Chang 6 section of the Qilicun field was formed in the Early Cretaceous (135 - 100 Ma) in the first stage, the initial filling period (135 - 120 Ma), and the second stage, the massive filling period (120 - 100 Ma). This study can provide some geological basis for oil exploration and development in the Qilicun field and adjacent areas.

Subject Areas

Petroleum Geology

Keywords

Fluid Inclusion, Homogeneous Temperature, Reservoir Formation, Chang 6 Oil Formation, Qilicun Oil Field, Ordos Basin

1. Introduction

Fluid inclusions are the "fossils" of the mineral growth process, which record the real palaeofluid information when the formation was formed, and their composition, physicochemical properties and existence state can reflect the relevant information of oil and gas formation [1]. In the field of petroleum geology, petrographic characterisation of fluid inclusions, microcalorimetry, fluorescence spectroscopy and laser Raman analysis are effective methods for recovering basin paleotherm, analysing basin evolution history, elaborating reservoir fluid properties, determining hydrocarbon formation and filling period [2]-[7]. The Ordos Basin is currently the largest oil-producing base in China, and the Chang 6 Formation of the Upper Triassic Yanchang Group is its main oil-rich formation, and is dominated by tight oil. The inclusions of the Chang 6 Formation of the Yanchang Group in different areas of the Ordos Basin have been studied in some detail by previous authors. Tang Jianyun, Cao Qing and Wang Naijun [8] [9] [10] considered the Chang 6 Formation to be a one-stage reservoir, corresponding to a time of formation between 125 and 100 Ma; Li Bo and Gao Zhendong [11] [12] considered it to be a two-stage reservoir, corresponding to a time of formation between 130 and 115 Ma and 108 and 80 Ma; other scholars' view was a three-stage reservoir [13], corresponding to a time of formation between 140 and In summary, there are still controversies about the formation time and period of the Chang 6 reservoir in the Yanchang Formation of the Ordos Basin, and previous studies mainly focus on the sedimentary centre of the lake basin during the Yanchang Formation period, while the formation time of the Chang 6 reservoir in the marginal part of the lake basin is rarely addressed. Although the Qilicun field has a total proven geological reserve of over 200 million tonnes of oil, studies on the formation of oil and gas accumulations are very weak, especially the timing of oil and gas reservoir formation has not been studied in the past.

The Qilicun oil field is located in Yan'an City, in the southeastern part of the northern slope of the Ordos Basin in Shaanxi Province (**Figure 1(a)**), and is the earliest exploration and development area in the Ordos Basin with a history of more than 100 years. The Chang 6 oil formation is its main oil-producing layer, and the submerged divergent river reservoir group at the front edge of the delta is developed (**Figure 1(b)**), with a total proven tight oil geological reserve of 225 million tonnes [14]. Previous studies in this field have focused on hydrocarbon source rock characteristics and oil source comparison [14] [15] [16], sedimentary phases and reservoir characteristics [17] [18] [19], with less attention paid to hydrocarbon reservoir formation. However, after years of depleted development, the field has gradually exposed the difficulties in stable production and the lack of favourable exploration blocks to deploy wells, and there is an urgent need to reconceptualise the formation conditions of the Chang 6 reservoir, of which the formation time and period of the reservoir is an important part. Therefore, this study is not only beneficial to the re-understanding of the formation process of oil and gas, but also important for the next step of oil exploration in this field.

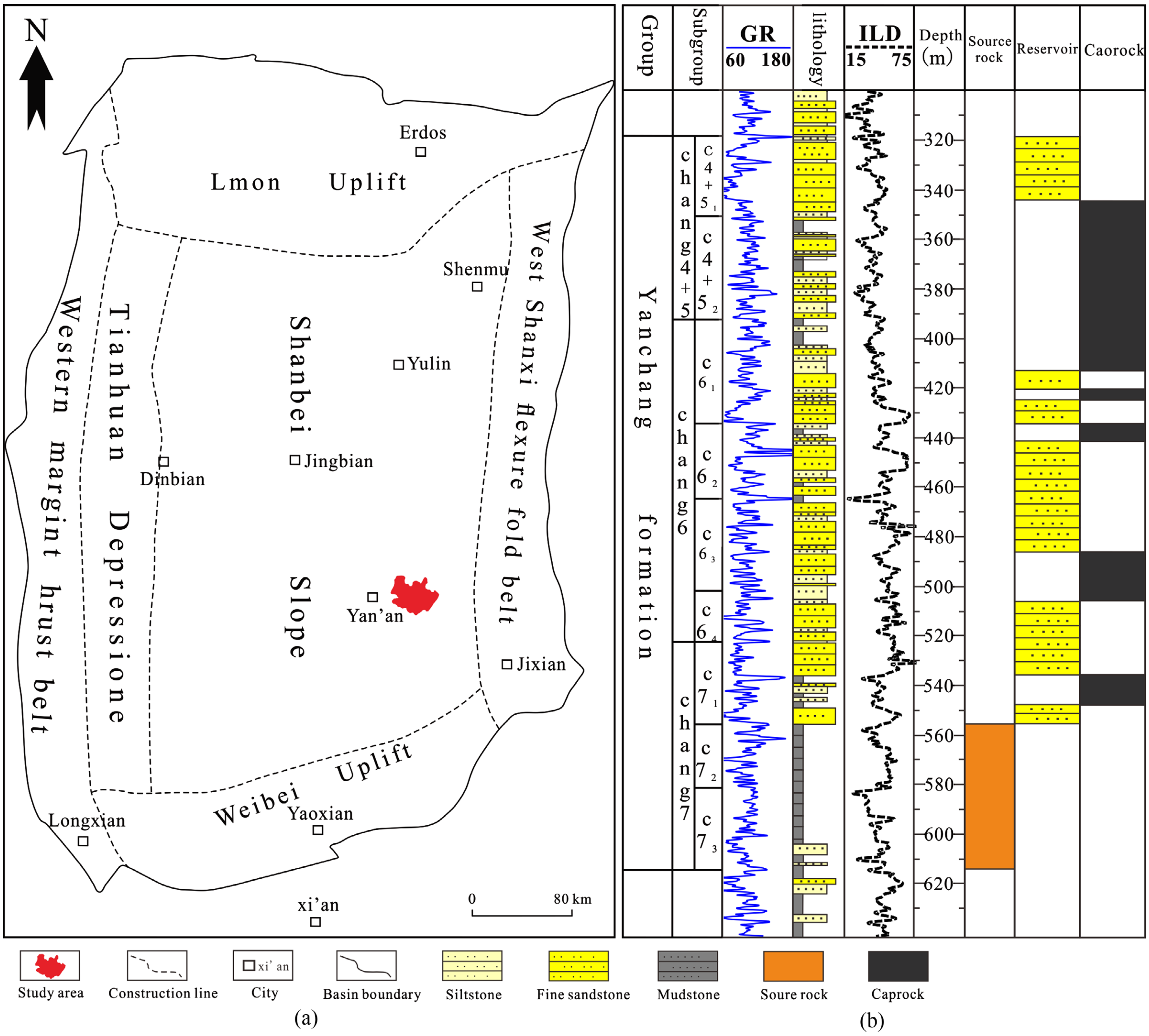

Figure 1. The division of structural units in ordos basin and the position of the study area and stratigraphic column of yanchang formation. (a) Division of basin tectonic units and location of study area; (b) Comprehensive histogram of Qilicun Yanchang Formation.

2. Characterisation of Fluid Inclusions in the Chang 6 Reservoir

2.1. Sample Collection and Processing

In this study, a total of 30 fluid inclusion thin sections were prepared from the core samples of four exploratory wells, DT033, DT036, DT038 and DT071, in the Qilicun field, for petrographic observation of fluid inclusions, fluorescence spectroscopy analysis and microtemperature measurement, etc. (Figure 2). The lithology was mainly fine sandstone and the depth was mainly distributed between 300 - 600 m. The rock samples were cored and ground to approximately 1 mm thick flakes and polished on both sides. For homogeneous temperature determination, a high level of thin section is required and the section needs to be

Figure 2. Sandstone samples from Qilicun oilfield, ordos basin.

pre-treated before testing. The surface is first cleaned with a small amount of acetone solution using a skimmed cotton pad and wiped back and forth to remove the organic material from the surface. The surface is then wiped several times with alcohol and finally scrubbed with deionised water. The main instruments used for fluid inclusion analysis were a Leica 07 optical microscope with blue fluorescence excitation, a GaiaFieldPro-V10 high light fluorescence spectroscopy imager, and a LinkamTHMS-G600 hot and cold bench with an accuracy of ±0.1˚C. All experiments were completed at Shaanxi Key Laboratory of Petroleum Accumulation Geology, Xi'an Shiyou University. The experimental procedures as well as the operating techniques strictly comply with the oil and gas industry standard "SY/T6010-2011 Microcalorimetry of fluid inclusions in sedimentary basins".

2.2. Inclusion Types and Characteristics

Fluid inclusions in the Chang 6 reservoir of the Yanchang Formation in the Qilicun oilfield are very well developed, mainly within quartz microfractures and to a lesser extent in feldspar grains, and are regularly distributed in strips, beads, clusters, and sporadic spots (Figure 3). According to the phase and composition characteristics of inclusions, they can be divided into pure brine inclusions, gas-bearing brine inclusions and hydrocarbon inclusions.

2.2.1. Pure Brine Inclusions

Pure brine inclusions are prevalent in the Chang 6 reservoir, mostly associated with gas-bearing brine inclusions, mainly transparent, non-bubbly, non-fluorescent, mainly in quartz grains and quartz healing microfractures, ranging in size from 3 to 10 μm (Figure 3(a) and Figure 3(b)), and mostly oval or irregular in shape.

2.2.2. Gas-Bearing Brine Inclusions

The gas-bearing brine inclusions are widely distributed in the Qilicun reservoir and appear transparent or light grey in transmitted light, not fluorescent; their diameters mainly range from 5 to 10 μm, with a wide range of gas-liquid ratios,

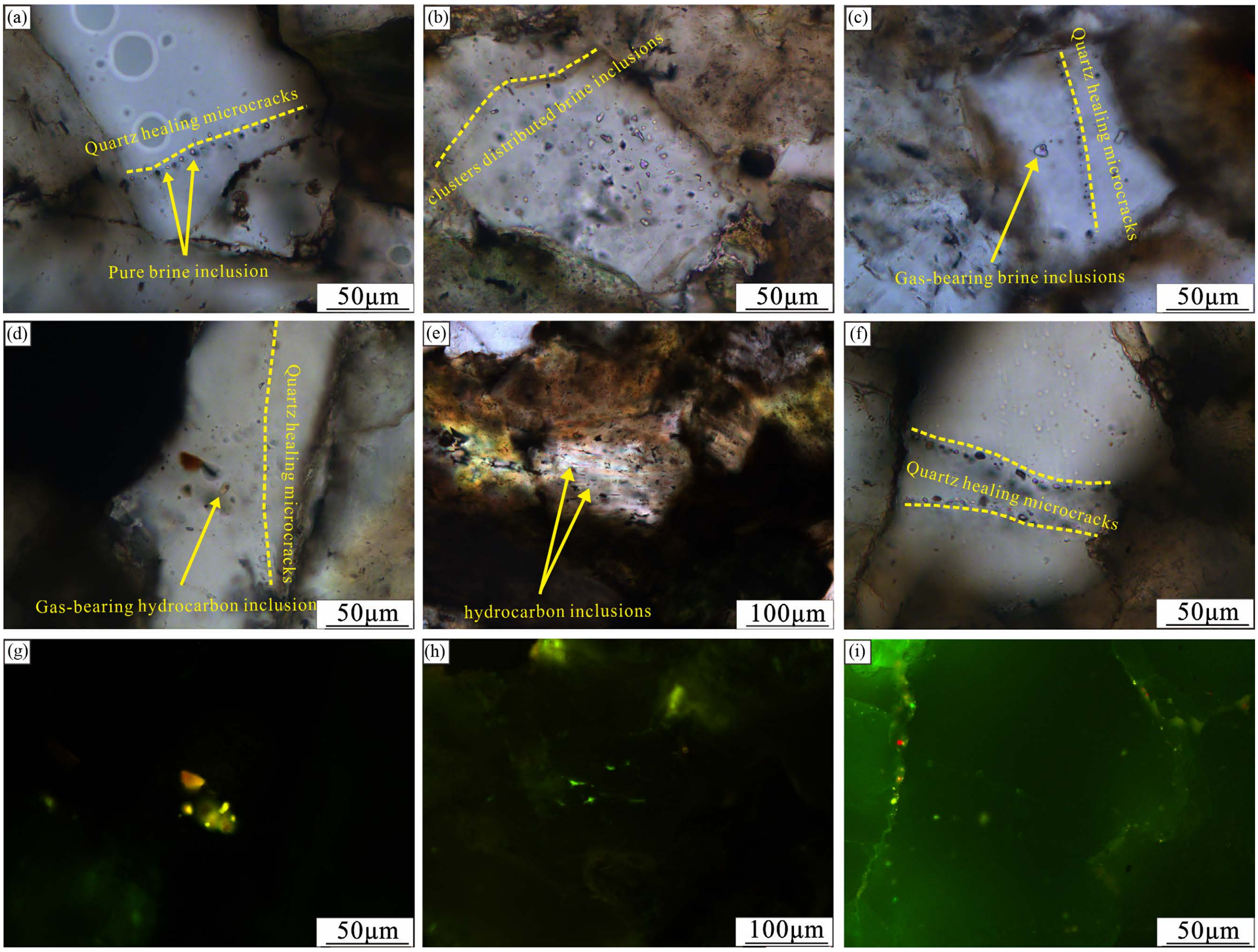

Figure 3. Microscopic characteristics of fluid inclusions in Chang 6 reservoir of Qilicun oilfield, ordos basin.

up to 3% - 20%; they are mostly distributed along quartz healing fractures in the form of beads, strips, sheets and scattered spots; their shapes are oval, elongated and irregular (Figure 3(b) and Figure 3(c)).

2.2.3. Hydrocarbon Inclusions

Hydrocarbon inclusions are mostly associated with brine inclusions (Figure 3(d) and Figure 3(e) and Figure 3(f)), and some hydrocarbon inclusions exist in bubbles (Figure 3(d)), which are between 3 and 8 μm in diameter, mainly scattered within quartz microfractures and feldspar grains; the difference in distribution between hydrocarbon inclusions and brine inclusions is more obvious, and hydrocarbon inclusions are more abundantly developed at the top of Chang 6; they are generally transparent or grey in transmitted light. The fluorescence colour of the inclusions can be observed to initially determine the maturity of the organic matter [20] [21], and the corresponding fluorescence colours from lowest to highest maturity are: red, orange, yellow, green, blue and blue-white. The hydrocarbon inclusions in the Qilicun field are yellowish green or green under fluorescence (Figure 3(g) and Figure 3(h) and Figure 3(i)); based on the maturity characteristics corresponding to the fluorescence of the inclusions, it is judged that the Chang 6 reservoir in the Qilicun field is in the mature evolutionary stage, and this result is consistent with studies on the degree of thermal evolution of organic matter in the area [22].

(a) Well DT036, pure brine inclusions distributed along healing fractures within quartz grains, Monopolarization, c 6_1, 198.12 m, 500×; (b) Well DT036, clustered brine inclusions within quartz grain fractures, Monopolarization, c 6_1, 198.12 m, 500×; (c) Well DT036, gas-liquid two-phase brine inclusions distributed along quartz healing microfractures, Monopolarization, c 6_1, 198.12 m, 500×; (d) Well DT033, gas-bearing hydrocarbon inclusions associated with quartz grains near healed microfractures, Monopolarization, c 6_1, 365.4 m, 500×; (e) Well DT033, liquid hydrocarbon inclusions within feldspar grains, Monopolarization, c 6_1, 317.51 m, 200×; (f) Well DT033, brine inclusions along fractures within quartz grains distributed brine inclusions with minor associated hydrocarbon inclusions, Monopolarization, c 6_2, 379.68 m, 500×; (g) Hydrocarbon inclusions fluorescing yellowish green, fluorescence, c 6_1, 365.4 m, 500×, in the same field of view as d; (h) Hydrocarbon inclusions fluorescing green, fluorescence, c 6_1, 317.51 m, 200×, in the same field of view as e; (i) Hydrocarbon inclusions fluorescing faint green, fluorescence, in the same field of view as f of hydrocarbon inclusions, fluorescent, c 6_2, 379.68 m, 500×.

3. Fluorescence Spectral Characteristics of Inclusions

Fluorescence spectroscopy of fluid inclusions is a non-destructive analytical method, and the spectrometer can record the different emission wavelengths of the fluorescent samples, thus achieving quantitative analysis of fluorescence intensity. The main peak wavelength of the spectrum (λ_{max}) is the emission wavelength corresponding to the maximum fluorescence intensity ($I_{max)}$ in the luminous sample point. λ_{max} can't identify the chemical components in the oil sample, but can determine the maturity of the oil. In general, the greater the maturity of the oil, the more small-molecule hydrocarbon content, the smaller the value of λ_{max}; conversely, the less small-molecule hydrocarbon content, the greater the value of λ_{max}. Therefore, hydrocarbons that undergo filling in the same phase should have the same or similar maturity and main peak wavelengths, and vice versa [23] [24].

Fluorescence spectroscopy analysis of selected fluorescence thin sections at different depths in the Chang 6 reservoir (**Figure 4**) showed that their λ_{max} ranged from 542.4 to 549.1 nm; fluorescence spectroscopy analysis of typical oil inclusions in the Qilicun field (**Figure 5**) showed that a set of values of λ_{max} mainly existed, ranging from 542.4 to 545.8 nm; the λ_{max} of fluorescence thin sections and oil inclusions were basically the same, indicating that The hydrocarbons have homologous characteristics and the maturity is the same, and the oil in the Chang 6 reservoir of the Qilicun field is a phase I filling.

(a) DT033, c 6_2,372.39 m long, fine sandstone with yellowish green fluorescent oil inclusions within quartz grains (a_1) and its fluorescence spectrum (a_2).

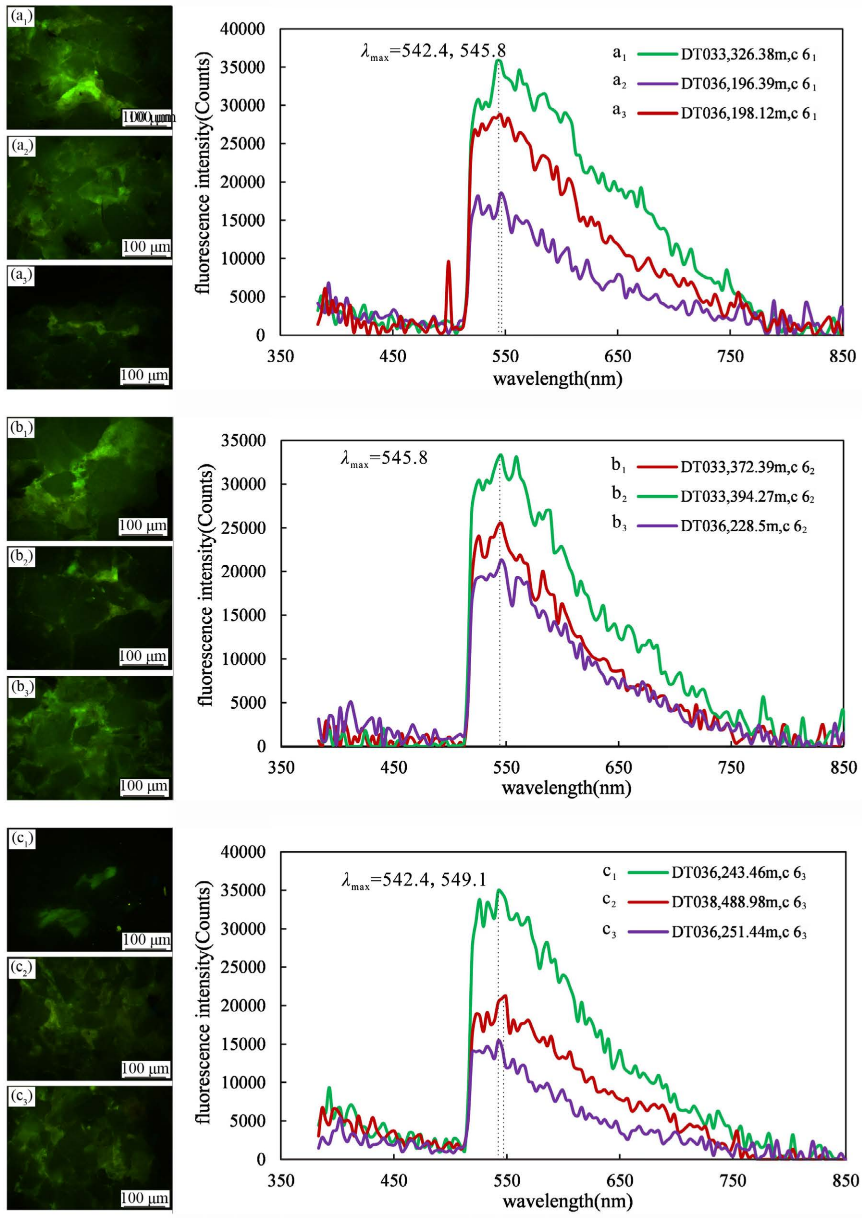

Figure 4. Fluorescence thin section and its corresponding fluorescence spectrum of Chang 6 member in Qilicun Oilfield.

(b) DT036, c 6_3, 243.46 m long, fine sandstone, yellowish green fluorescent oil inclusions within quartz grains (b_1) with its fluorescence spectrum (b_2).

(c) DT033, c 6_1, 365.4 m long, fine sandstone, yellowish green fluorescent oil inclusions in quartz grains (c_1) with its fluorescence spectrum (c_2).

4. Homogeneous Temperature and Salinity Distribution Characteristics of the Envelope

4.1. Homogeneous Temperature Distribution Characteristics

Inclusion homogeneous temperature and salinity characteristics are one of the most important research elements in determining the reservoir formation period

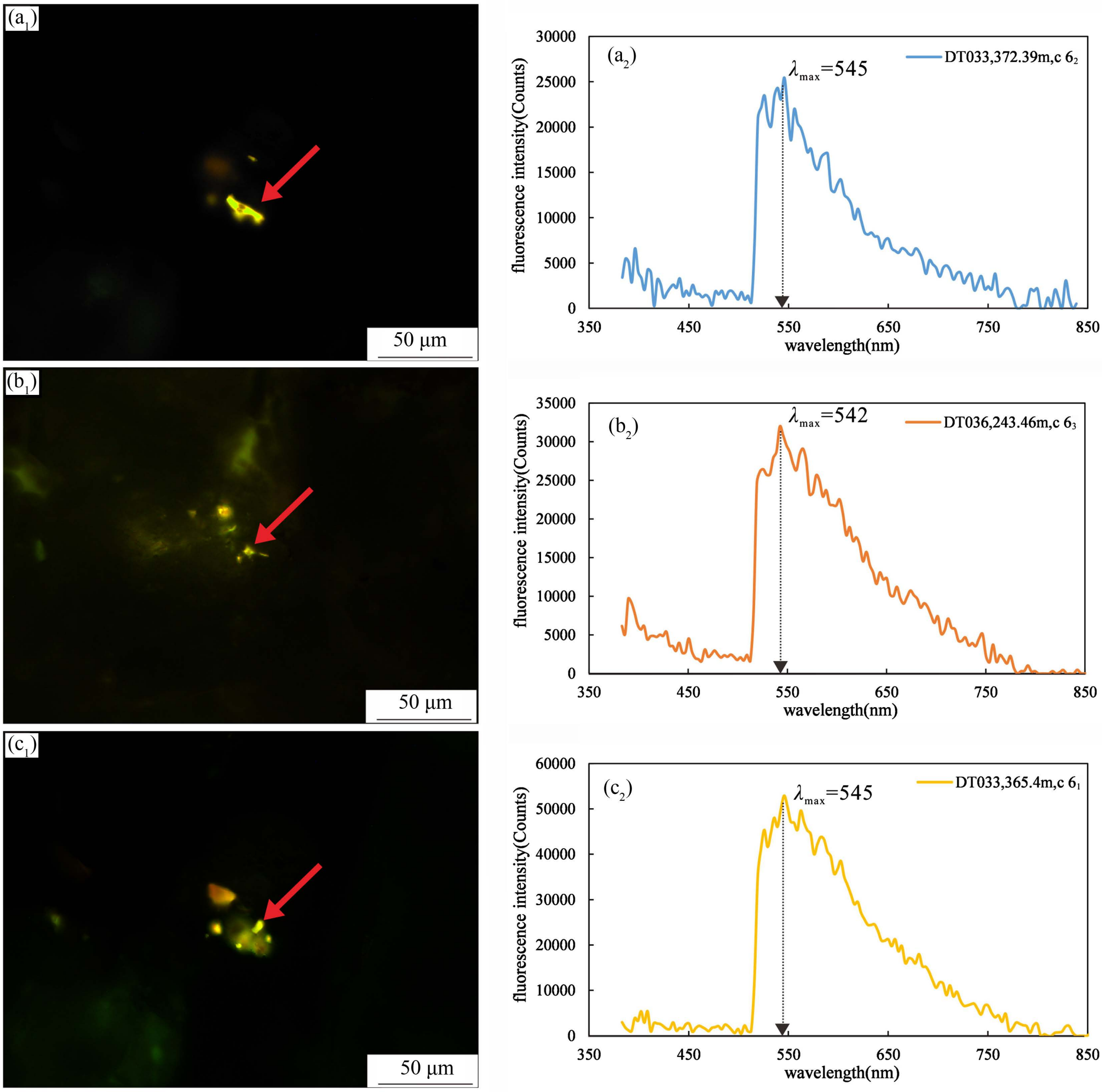

Figure 5. Oil inclusions and their corresponding fluorescence spectra in Qilicun oilfield.

and reservoir age, and are an important basis for comprehensive analysis of the reservoir formation period and reservoir age [5] [6] [7] [8] [9] [25]. The homogeneous temperature of inclusions is the minimum temperature required for the conversion of gas-liquid inclusions into a homogeneous phase. The homogeneous temperature of brine inclusions coeval with hydrocarbon inclusions in a reservoir can approximately represent the formation temperature when oil and gas filling occurs. As hydrocarbon inclusions contain organic hydrocarbons, the temperature homogenisation is often not representative of the minimum temperature at which oil and gas injection occurs, therefore, brine inclusions co-occurring with hydrocarbon inclusions are usually selected for homogenisation experiments.

A total of 249 inclusions distributed within quartz grains and quartz healed microfractures were selected for temperature measurement, and the test results show that (**Figure 6**): the overall range of measured mean temperature of fluid inclusions in the Chang 6 reservoir in the Qilicun field is between 70˚C and 140˚C, with a wide overall span; the distribution of mean temperature of inclusions is bimodal, with the first peak being low, between 90˚C and 95˚C, and the second peak being more pronounced, between 110˚C and 110˚C. The first peak is low, between 90˚C and 95˚C, and the second peak is more pronounced, between 110˚C and 115˚C. From an overall perspective, the main peak of the mean temperature is between 100˚C and 120˚C, which can be considered as the formation temperature when the oil and gas is heavily filled, and represents the main reservoir formation period of the oil and gas.

4.2. Salinity Distribution Characteristics

The salinity characteristics of an inclusion can be indicative of the physicochemical properties and origin of the fluid and can be calculated from the freezing point temperature of the brine inclusion [26]. In this study, the salinity of fluid inclusions in the Qilicun field was calculated using the empirical formula method. The results show (**Figure 7**) that the overall range of salinity of fluid inclusions in the Chang 6 reservoir in the Qilicun Oilfield is distributed between 0.88% and 18%, with an overall low salinity, indicating that the fluid inclusions were formed in a freshwater or brackish water environment; the distribution trend shows that there are two peaks in the salinity distribution approximation,

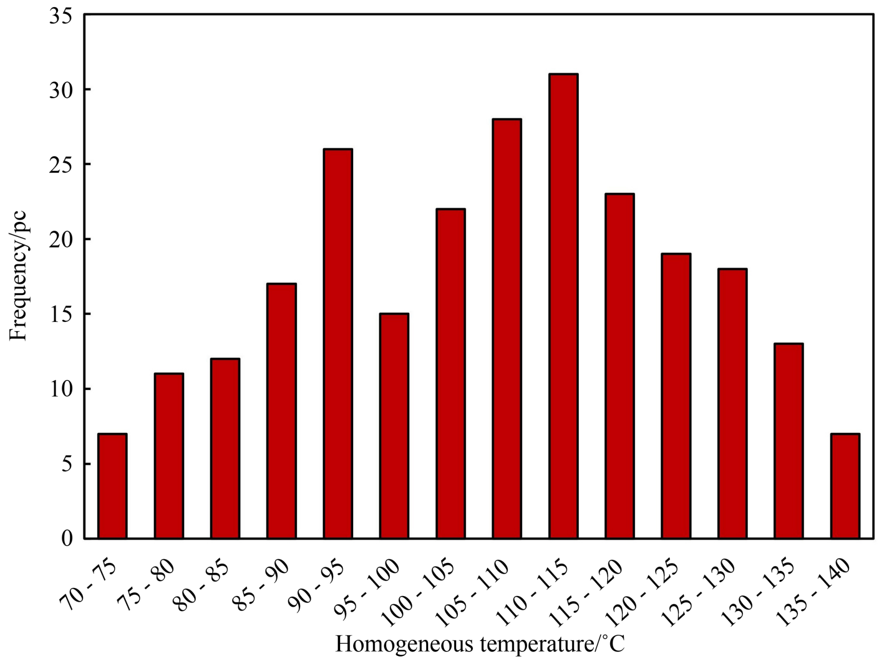

Figure 6. Histogram of homogenization temperature of inclusions in Chang 6 member of Qilicun oilfield.

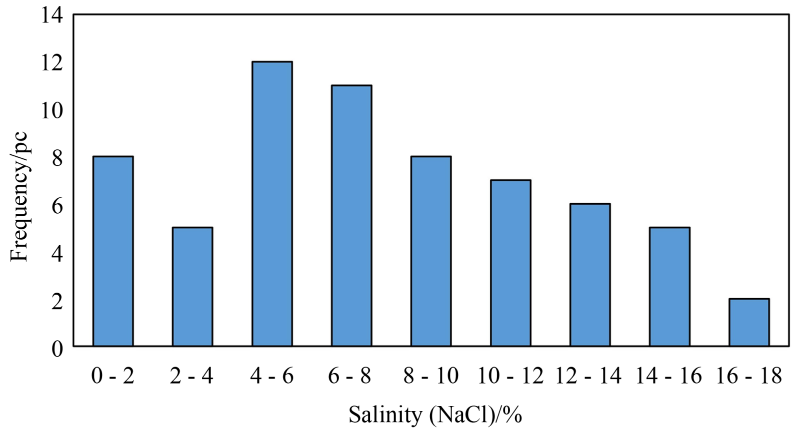

Figure 7. Histogram of salinity of inclusions in Chang 6 member of Qilicun oilfield.

0.88% to 2% and 4% to 8%, respectively. The second peak is more obvious, with salinity in the range of 4% - 8%, which can be considered the main peak; in terms of variation characteristics, the overall salinity shows a trend of decreasing, then increasing and then decreasing, with an overall single peak, reflecting that the Qilicun field is a Phase I fluid activity event.

5. Burial-Thermal Evolution History and Reservoir Timing

Fluid inclusions are a scientific and effective method in reservoir formation studies, especially when combined with the burial-thermal evolution history and fluid inclusions thermometry to determine the reservoir formation time, which has become an effective means to determine the reservoir formation age.

5.1. Recovery of Stripping Volumes at the End of the Early Cretaceous in the Qilicun Oil Field

Since the Triassic, the Qilicun oil field has experienced relatively frequent geological and tectonic movements. The overall expression is four phases of uplift and denudation: minor uplift and denudation at the end of the Triassic, denudation at the end of the Early Jurassic, denudation at the end of the Late Jurassic and denudation at the end of the Cretaceous; since the Cenozoic, the basin has generally shown continuous sedimentary subsidence [10]. For the late Cretaceous uplift denudation in the Qilicun area, the author used the sonic time difference method to recover the denudation thickness. In normally deposited compacted mud shales, the amount of denudation in the strata can be deduced using the relationship between Δt ¾H:

$$\Delta t = \Delta t_0 e^{-kH}$$

where H is the depth of burial, m; Δt is the acoustic time difference at depth H, μm/s; Δt_0 is the acoustic time difference at the surface, taking a value of 620 μm/s, and k is the slope of the normal compaction curve. If the strata are normally compacted and deposited, the sonic time difference of the mudstone varies exponentially and continuously, and when the strata have undergone uplift stripping, the sonic time difference value will deviate from the original trend line. Therefore, the change of acoustic time difference of mudstone is discontinuous for the strata that have been denuded. The trend line of mudstone compaction can be extended above the unconformity surface of the strata to the paleosurface at Δt_0. The absolute depth between the unconformity surface and the paleosurface is the amount of paleodenudation of the strata [27]. For the Late Cretaceous tectonic movement, the unconformity surface is the base of the Quaternary stratigraphy. The author took DT016, DT036 and DT071 wells as examples, read the values of the sonic time difference logging curves, paid attention to selecting pure mudstone sections greater than 2 meters in the shallow undeveloped overpressure strata, and produced compaction curves based on the sonic time difference of the read mudstone to recover the denudation thickness of the Late Cretaceous (**Figure 8**). Synthesizing the results of previous research [28] [29] and the author's calculations of denudation thickness, the denudation in the study area is 40 - 60 m, 120 - 160 m, 240 - 280 m and 1605 - 1712 m for the late Triassic, late Middle Jurassic, late Jurassic and late Cretaceous.

5.2. Determination of the Timing and Timing of the Formation of the Chang 6 Reservoir

The main method currently used to determine the reservoir formation time using fluid inclusions is to project the homogeneous temperature data onto the burial and thermal evolution history map of a single well in the study area, and the geological time corresponding to the projection of the homogeneous temperature on the map can be used to comprehensively determine the oil and gas filling time [2] [30] [31] [32] [33]. In this study, the burial history of a single well in the study area was simulated using Petromod software. The parameters

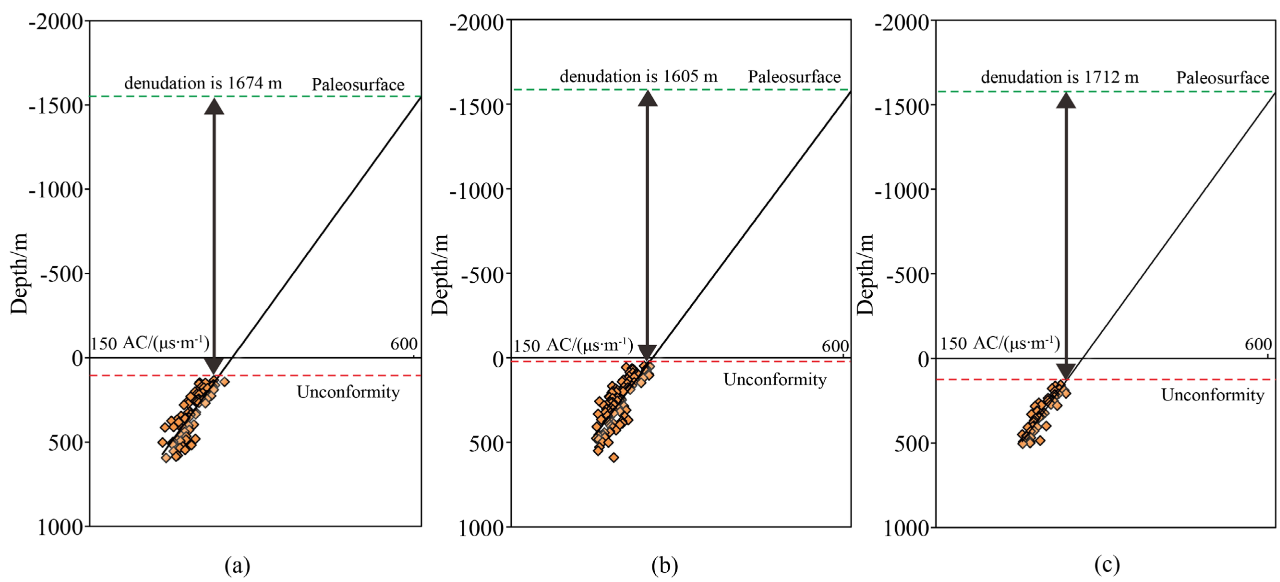

Figure 8. Estimation of stratum denudation thickness at the end of cretaceous in Qilichun oilfield. (a) DT016; (b) DT036; (c) DT071.

required for the simulation were basin palaeo-geothermal flow (HF) values obtained with reference to previous research results [25] [28] [34], palaeo-water depth was set to 0, and global sea level temperature (SWIT) was automatically generated by the software based on the latitude and longitude of the Qilicun oilfield. The simulation was based on the calculation of formation stripping volume and combined with the measured vitrinite reflectance (Ro) to calibrate the single well simulation results to ensure the accuracy of the simulation results (**Figure 9**).

The simulation results show (**Figure 10**) that the Chang 6 section of the Qilicun field is a one-stage reservoir, spanning from the early Early Cretaceous (135 Ma) to the end of the Early Cretaceous (100 Ma), a continuous filling process over a period of 35 Ma. Based on the homogeneous temperature and salinity analysis of the inclusions, it is believed that there are two stages of oil and gas formation in the Qilicun field. The first stage is the initial filling period, which lasted from the early Early Cretaceous (135 Ma) to the middle Early Cretaceous (120 Ma) for a period of about 15 Ma, corresponding to a homogeneous temperature of 70˚C - 100˚C and a salinity of 0.88% - 2%. From the thermal evolution history of hydrocarbon source rocks, the Ro value of early to middle Early Cretaceous hydrocarbon source rocks was 0.5% - 0.7% at this time, which had

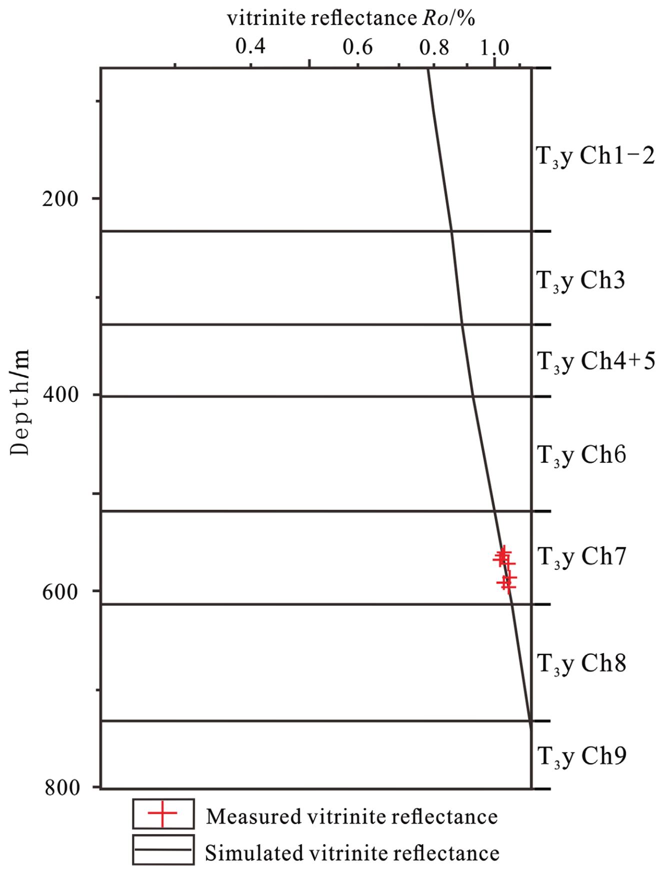

Figure 9. Relationship between measured vitrinite reflectance and simulated vitrinite reflectance in Qilicun oilfield.

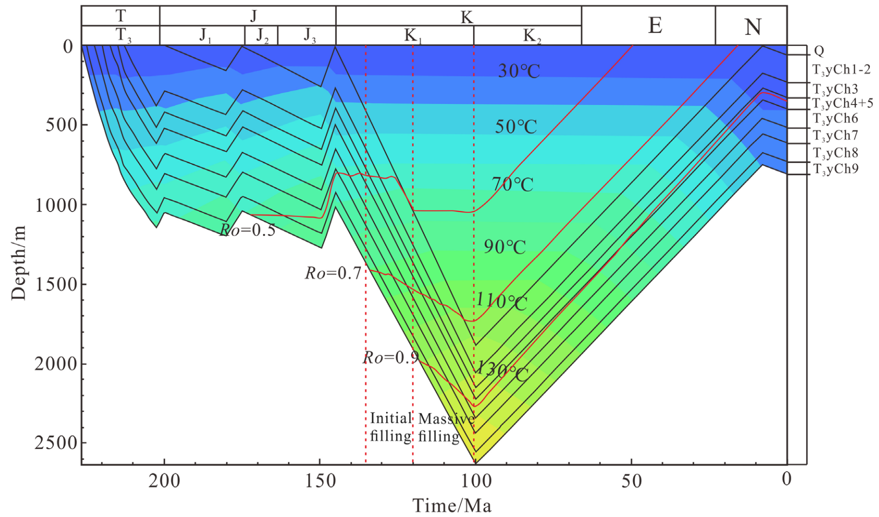

Figure 10. Burial and thermal histories and accumulation time of Chang 6 Reservoir in Qilicun oilfield.

reached the hydrocarbon generation threshold [35]. The hydrocarbon source rocks began to produce hydrocarbons and fill the Chang 6 reservoir, and yellowish green fluorescent inclusions are seen under the microscope; the second stage is the massive filling period (main reservoir formation period), which lasted from the middle Early Cretaceous (120 Ma) to the end of the Early Cretaceous (100 Ma) for about 20 Ma, corresponding to a homogeneous temperature of 100˚C - 140˚C. At this time, the Ro values of the middle and late Early Cretaceous were between 0.7% and 0.9%. The hydrocarbon source rocks began to produce hydrocarbons in large quantities and were continuously filled into the Chang 6 reservoir, microscopically as green fluorescent inclusions. After 100 Ma, due to regional tectonic activity, the stratigraphic temperature ceased to increase with time and hydrocarbon production and discharge activities of the hydrocarbon source rocks ceased, thus ending the main hydrocarbon reservoir formation period.

6. Conclusions

1) A large number of brine inclusions, gas-liquid two-phase brine inclusions and a small amount of oil inclusions are developed in the Chang 6 reservoir of the Yanchang Formation in the Qilicun Oilfield of the Ordos Basin, and the fluorescence colour of the oil inclusions is mainly yellowish green and green, indicating that the Chang 6 reservoir is in a mature evolutionary stage.

2) The main peak of fluorescence spectra of fluorescence flakes and typical oil inclusions are between 542.4 - 549.1 nm, indicating that the hydrocarbon maturity of the Chang 6 reservoir is basically the same, and it is in the first stage of filling.

3) The brine inclusions have a wide range of uniform temperature distribution, with an overall bimodal distribution; the uniform temperature is distri-

buted from 70˚C to 140˚C and the main body is distributed from 100˚C to 120˚C; the salinity is distributed from 0.88% to 18%, also approximating two peaks, with the main peak peaking at 4% to 8%.

4) The stripping thickness at the end of the Early Cretaceous in the Qilicun field recovered using the acoustic time difference method is 1605 - 1712 m. Integrating the burial-thermal evolution history of the Chang 6 reservoir in the Qilicun field, the hydrocarbon source rock thermal evolution history and the inclusions of homogeneous temperature data, it is inferred that the Chang 6 reservoir in this area is mainly a Phase I formation (135 - 100 Ma), divided into an initial filling period (135 - 120 Ma) and a massive filling period (120 - 100 Ma).

Conflicts of Interest

The authors declare no conflicts of interest.

References

[1] Lu, H.Z. (2004) Fluid Inclusion. Science Press, Beijing.

[2] Zhao, J.Z. (2002) Hydrocarbon Inclusion Analysis: Application in Geochronological Study of Hydrocarbon Accumulation. *Geology Geochemistry*, **30**, 83-89.

[3] Pan, L.Y., Ni, P., Ou, G.X., *et al.* (2006) Application of Organic Inclusion Study in Petroleum Geology—Conception, Classification, Formation Mechanism and Significance. *Bulletin of Mineralogy*, *Petrology and Geochemistry*, **25**, 19-28.

[4] Li, K., George, S.C., Cai, C., *et al.* (2019) Fluid Inclusion and Stable Isotopic Studies of Thermochemical Sulfate Reduction: Upper Permian and Lower Triassic Gas Fields, Northeast Sichuan Basin, China. *Geochimica et Cosmochimica Acta*, **246**, 86-108. https://doi.org/10.1016/j.gca.2018.11.032

[5] Zhan, W.Z. and Kelsang, W.D. (2018) Fluid Inclusion Analysis for Ezongcuo Area of Upper Triassic Formation in Qiangtang Basin. *Fault-Block Oil and Gas Field*, **25**, 5.

[6] Zhao, H.Q., Chen, C.L., Chen, X.M., *et al.* (2018) Coupling Relationship between Diagenesis and Hydrocarbon Charging in Upper 3rd Member of Eogene Shahejie Formation of Kenli 10-4 Oilfield. *Fault-Block Oil and Gas Field*, **25**, 5.

[7] Chen, L., Xu, C.G., Yang, H.F., *et al.* (2017) Characteristics of Cenozoic Fluid Inclusions and Accumulation Period in Southern Slope of Huanghekou Sag. *Fault-Block Oil and Gas Field*, **24**, 5.

[8] Cao, Q., Zhao, J.Z. and Liu, Y.Q. (2013) Fluid Inclusions of Chang2 and Chang6 Sections in Yanchang Formation, Panlong Area, Ordos Basin. *Petroleum Geology and Experiment*, **35**, 384-388.

[9] Wang, N.J., Zhao, J.Z., *et al.* (2010) Determination of the Age of Accumulation by Fluid Inclusion with an Example from Triassic Yanchang Formation in the Xiasiwan Area, Ordos Basion. *Journal of Lanzhou University* (*Natural Sciences*), **46**, 22-25.

[10] Tang, J.Y., Zhang, G., Shi, Z., *et al.* (2019) Characteristics of Fluid Inclusions and Hydrocarbon Accumulation Stages of Yanchang Formation in Fengfuchuan Area, Ordos Basin. *Lithologic Reservoirs*, **31**, 20-26.

[11] Gao, Z.D., Zhao, J.Z., Cao, Q., *et al.* (2008) Geochronological Analysis of Oil Accumulation in Triassic Yanchang Formation, Ordos Basin. *Northwestern Geology*, No. 3, 92-98.

[12] Li, B., Cui, J.P., Li, Y., *et al.* (2021) Hydrocarbon Accumulation Phases of Yanchang Formation in Wuqi Area, Yishan Slope. *Lithologic Reservoirs*, **33**, 21-28.

[13] Fu, J.H., Liu, G.D., Yang, W.W., *et al.* (2013) A Study of the Accumulation Periods of Low Permeability Reserivor of Yangchang Formation in Longdong Area, Ordos Basin. *Earth Science Frontiers*, **20**, 125-131.

[14] Zhao, J.Z., Meng, X.G. and Han, Z.H. (2020) Near-Source Hydrocarbon Accumulation: Geochemical Evidence of Lacustrine Crude Oil from the Member 6 of Yanchang Formation, Eastern Margin of Ordos Basin. *Acta Petrolei Sinica*, **41**, 1513-1526.

[15] Bai, Y.B., Zhao, J.Z., Huang, Y.J. and Han, Z.H. (2022) Excellent Source Rocks Found along the Margin of a Large Lacustrine Basin: Case Study from the Ordos Basin, China. *Journal of Petroleum Science and Engineering*, **214**, Article ID: 110569. https://doi.org/10.1016/j.petrol.2022.110569

[16] Cui, L., Liao, X., Zhou, L., *et al.* (2019) Paleogeomorphic Influence on Facies Characteristics of Braided Delta and Reservoir Prediction—An Example from L Oilfield in Bohai Bay Basin. *Journal of Geoscience and Environment Protection*, **7**, 195-205. https://doi.org/10.4236/gep.2019.78014

[17] Cui, W.L., Han, H.F., Zhang, Y., *et al.* (2019) Reservoir Microscopic Characteristics and Oil Content of Chang 6 Tight Sandstone in Lijiachengze Area, Jingbian Oilfield. *Petroleum Geology and Experiment*, **41**, 390-397.

[18] Wang, Q.Y., Yang, W., Ge, Y.J., *et al.* (2021) Diagenetic Responses to Delta Front-Lacustrine Depositional Microfacies and Implications for Tight Reservoir Quality Differences in the Yanchang Formation, Western Ordos Basin. *Acta Sedimentologica Sinica*, **39**, 841-862.

[19] Deng, X.Q., Fu, J.H. and Yao, J.L. (2011) Sedimentary Facies of the Middle-Upper Triassic Yanchang Formation in Ordos Basin and Breakthrough in Petroleum Exploration. *Journal of Palaeogeography*, **13**, 443-455.

[20] Eadington, P.J., Hamilton, P.J. and Bai, G.P. (1991) Fluid History Analysis—A Prospect Evaluation. *The APPEA Journal*, **31**, 282. https://doi.org/10.1071/AJ90022

[21] Zhao, Y.J. and Chen, H.H. (2008) The Relationship between Fluorescence Colors of Oil Inclusions and Their Maturities. *Earth Science—Journal of China University of Geosciences*, **33**, 6.

[22] Han, Z.H. (2020) Study on Source Rock and Reservoir Forming Dynamic of Chnag7-Member in Qlichun Oilfield, Ordos Basin. *Xi'an Shiyou University*, **30**, 7.

[23] Li, C.Q., Chen, H.H. and Liu, H.M. (2010) Identification of Hydrocarbon Charging Events by Using Micro-Beam Fluorescence Spectra of Petroleum Inclusions. *Earth Science—Journal of China University of Geosciences*, **35**, 657-662.

[24] Si, S.H., Chen, H.H., Yuan, B.L., *et al.* (2010) Identification of Hydrocarbon Charging Events by Using Fluorescence Spectrum Multiparameter of Oil Inclusions: A Case Study of Carboniferous in Bashituo Structural Belt of Markit Slope of Tarim Basin. *Marine Origin Petroleum Geology*, **35**, 657-662.

[25] Ren, Z.L., Zhang, S., Gao, S.L., *et al.* (2007) Tectonic Thermal Evolution History of Ordos Basin and Its Significance in Reservoir Formation and Mineralization. *Science in China Press*, No. S1, 23-32.

[26] Mi, J.K. (2003) Migration and Accumulation Characters of the Upper Paleozoic Gas Reservoir in Ordos Basin. Master's Thesis, Chinese Academy of Science (Guangzhou Institute of Chemistry), Guangzhou.

[27] Liu, Y.R. (2015) Correction of Erosion Thickness of Strata Calculated by Acoustic Time Difference. *Complex Hydrocarbon Reservoirs*, No. 2, 1-6.

[28] Chen, R.Y., Luo, X.R., Zhao, W.Z., *et al.* (2007) Thermal Anomaly and Thermal Evolution of Source Rocks in Mesozoic, Ordos Basin. *Petroleum Exploration and Development*, No. 6, 658-663.

[29] Weng, W.F., Wang, J.Q., Zhang, R.R., Chen, H. and Gui, X.J. (2011) Denudation Thickness Estimation of Sedimentary Formation in Ordos Basin by Acoustic Logging Information. *Xinjiang Petroleum Geology*, **32**, 143-146.

[30] Liu, J.L., Liu, K.Y. and Gui, L.L. (2019) Fluid Inclusion Characteristics and Hydrocarbon Charge History in the Upper Paleozoic, Central Ordos Basin. *Journal of China University of Petroleum* (*Edition of Natural Science*), **43**, 13-24.

[31] Liu, R.C., Ren, Z.L., Ma, K., *et al.* (2019) Classification of Hydrocarbon Accumulation Phases of Yanchang Formation in Southern Ordos Basin. *Geoscience*, **33**, 1263-1274.

[32] Han, Z.H., Zhao, J.Z. and Chen, M.N. (2020) Fluid Inclusion Characteristics and Hydrocarbon Accumulation Period of He8 Member Reservoir in the Western Area of Sulige Gasfield. *Journal of Xi'an Shiyou University* (*Natural Science Edition*), **35**, 18-27.

[33] Cao, Q., Gao, J.M., Fan, L.Y., *et al.* (2015) Characteristics and Significance of Fluid Inclusions in Upper Paleozoic of Southwest Ordos Basin. *Natural Gas Geoscience*, **26**, 2245-2253.

[34] Zhao, G.P. (2017) Characterization of Fluid Inclusions and Timing of Gas Accumulation in Upper Paleozoic Reservoirs of Hangjinqi Area, Ordos Basin. *Oil and Gas Geology*, **38**, 905-912.

[35] Wu, L.Y. and Gu, X.Z. (1986) The Application of Pyrolysis Technique in Source Rock Research. *Acta Petrolei Sinica*, No. 2, 13-19.